

## Infrared multispectral detection using Si/Si<sub>x</sub>Ge<sub>1-x</sub> quantum well infrared photodetectors

D. Krapf, B. Adoram, J. Shappir, and A. Sa'ar<sup>a)</sup>

*Department of Applied Physics, The Fredi and Nadine Herrmann School of Applied Science, The Hebrew University of Jerusalem, Jerusalem 91904, Israel*

S. G. Thomas, J. L. Liu, and K. L. Wang

*Department of Electrical Engineering, University of California at Los Angeles, California 90095-1594*

(Received 3 August 2000; accepted for publication 21 November 2000)

A modified *p*-type Si/SiGe quantum well infrared photodetector for multispectral infrared imaging applications is demonstrated. In order to improve the detector's performances we have used a SiGe emitter and a low-temperature wet passivation process that give rise to a reduced dark current, even at relatively high bias voltages. Multispectral photoresponse at the long, mid and short wavelength infrared atmospheric windows was observed. The response peaks are assigned to the various classes of intervalence band transitions in the quantum wells and in the SiGe emitter layers. © 2001 American Institute of Physics. [DOI: 10.1063/1.1343498]

Midinfrared multispectral imaging is a major goal in modern thermal imaging systems. In principle, using the *n*-type GaAs based quantum well infrared photodetectors (QWIPs) technology<sup>1-4</sup> one can design a multispectral detector by monolithically integrating several stacks of single-wavelength QWIPs.<sup>5,6</sup> However, several problems limit the applicability of this approach. For example, multicontact detectors (i.e., more than two contacts per detector) are not compatible with the current multiplexing technology. In addition, the GaAs based QWIP technology cannot be used for short wavelengths infrared (SWIR) detection so that alternative technologies should be used if imaging at this spectral window is required.

An alternative approach, of using *p*-type QWIPs, can also be employed for multispectral detection.<sup>7-11</sup> In this case, there are several classes of inter-valence optical transitions that can be utilized for multispectral detection. The first class is related to intersubband transitions (ISTs) between heavy hole (HH) states of the quantum well (QW) while the second class is related to intervalence transitions (IVTs) between the ground HH state and mixed spin split-off (SO) and light hole (LH) states.<sup>12</sup> Over the recent years there have been several reports on *p*-type QWIPs.<sup>7-11</sup> In most cases, it was found that a relatively high dark current on one hand and a limited number of spectral response windows on the other hand, limit the effectiveness of this approach. In this letter we show that, using a modified structure of *p*-type Si/SiGe QWIP,<sup>9-11</sup> one can solve most of these problems and fabricate a good quality QWIP for detection at both long-wavelength IR (LWIR), midwavelength IR (MWIR) as well as SWIR spectral windows.

The SiGe QWIP used for our study was grown by molecular beam epitaxy on a high resistivity (1500 Ω cm) *n*-type (100) Si substrate. The structure consists of 20 periods of SiGe/Si QWs. Each period consists of a 30-Å-wide Si<sub>0.77</sub>Ge<sub>0.23</sub> QW, boron (*p* type) doped to a level of 9.6

× 10<sup>11</sup> cm<sup>-2</sup>, and a 500 Å undoped Si barrier. In addition, a 300-Å-wide Si<sub>0.77</sub>Ge<sub>0.23</sub> emitter layer, *p*-doped to a level of 4 × 10<sup>18</sup> cm<sup>-3</sup>, was grown on top of the QWs. The whole structure is capped with 5000 Å top and bottom *p*<sup>++</sup> Si layers (*p* = 3 × 10<sup>19</sup> and 1 × 10<sup>19</sup> cm<sup>-3</sup>, respectively). For detector characterizations, the sample was processed into a 100-μm-diam mesa structure using standard photolithography and wet chemical etching. Al metallization was used for top and bottom ohmic contacts. The edge of the sample was polished in 45° to allow light coupling in various polarization angles.

We would like to point out several differences between the QWIP structure used for our study and previously reported SiGe QWIPs.<sup>9-11</sup> First, the use of lightly doped *n*-type Si substrate forms a reverse biased *p-n* junction between the bottom *p*-doped contact layer and the substrate. However, most of the depletion layer generated by this junction extends into the lightly doped substrate thus preventing parasitic substrate resistance contribution to the device as well as free carrier absorption in the substrate. Second, in order to reduce the relatively large dark current, usually measured for *p*-type SiGe QWIPs, we have used a SiGe emitter rather than Si emitter (as routinely done in previous reports). The heavily doped, 300-Å-wide, Si<sub>0.77</sub>Ge<sub>0.23</sub> layer (which is well below the critical thickness<sup>13</sup>) serves as an emitter with a practically ohmic contact to the top *p*<sup>++</sup> Si contact layer. However, the SiGe emitter forms a Schottky-type contact to the SiGe multiple quantum well (MQW) region in a similar manner to what is routinely done in GaAs QWIPs. As a result, an energy barrier is formed between the SiGe emitter and the first silicon barrier of the MQW. This barrier is expected to reduce the dark current of the device, particularly at low temperatures. Finally, we would like to point out a technological advantage of using the Si/SiGe material system that does not exist for other semiconductors. In a previous report (using the current sample) we found that thermal treatments up to 750 °C do not cause degradation of the optical properties of the structure.<sup>14,15</sup> As a result, prior to metallization, we were able to perform a wet thermal oxidation

<sup>a)</sup>Electronic mail: saar@vms.huji.ac.il

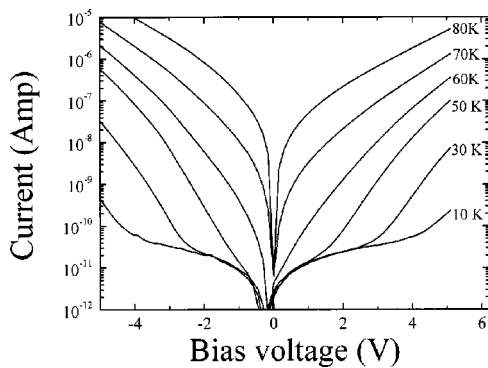


FIG. 1. Dark current–voltage characteristics of the shielded SiGe QWIP at various temperatures.

process to the SiGe QWIP that results in a good passivation of the device. Notice that the lack of a good passivation process for GaAs based devices and for previously reported SiGe QWIPs<sup>9</sup> could be another reason for device degradation and a relatively high dark current.

For dark current measurements the sample was placed in a shielded cryostat. Fig. 1 shows the current–voltage ( $I$ – $V$ ) characteristics at various temperatures. For a bias voltage of 5 V, the dark current is about 100 pA at 10 K and 1  $\mu$ A at 70 K. These values of the dark current are comparable to GaAs QWIPs<sup>1</sup> even at relatively high bias voltages. Let us point out that the asymmetry of the  $I$ – $V$  (i.e., the lower dark current for positive voltages) is expected in our structure since the emitter is made of SiGe while the collector is made of silicon.

The photocurrent response of the SiGe QWIP is shown in Fig. 2(a). Measurements were taken at 10 K using a Fourier transform infrared spectrometer (Perkin-Elmer system 2000) with the QWIP as an external detector. Four photocurrent peaks, at 1300, 1800, 2500, and a broad peak at around 4000  $\text{cm}^{-1}$  are clearly observed. The first three peaks are

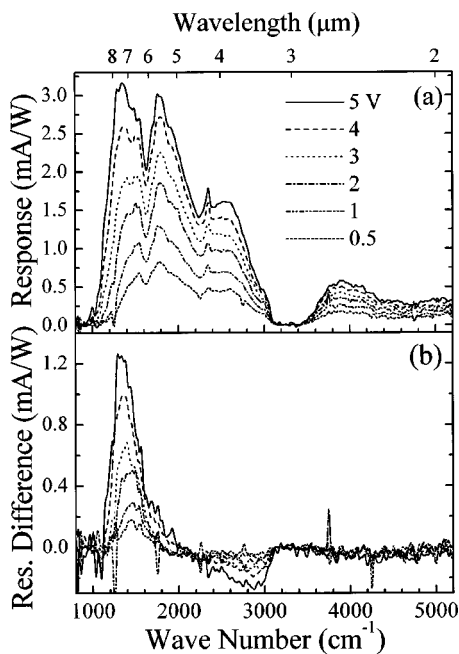


FIG. 2. (a) The spectral responsivity of the SiGe QWIP for various bias voltages measured for  $p$ -polarized (TM) IR beams. (b) The response difference between  $p$ - and  $s$ - polarized IR beams for various bias voltages.

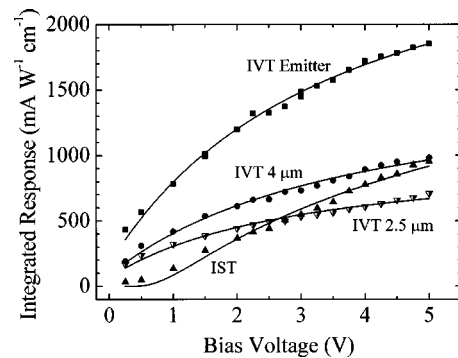


FIG. 3. The integrated response vs the bias voltage for the emitter (squares), IVT at 4  $\mu\text{m}$  (circles), IST (up triangles) and IVT at 2.5  $\mu\text{m}$  (down triangles) response peaks. The solid lines represent the best fits of the experimental data to the integrated response model.

well correlated with our previous IR-absorption measurements (see Fig. 1 in Ref. 14) and are assigned to HH1 $\rightarrow$ HH2 IST in the QWs, HH $\rightarrow$ (SO+LH) IVT in the SiGe emitter and HH1 $\rightarrow$ (SO+LH)1 IVT in the QWs, respectively. The assignment of these transitions is based on previous IR absorption measurements and Raman spectroscopy.<sup>14,15</sup> The weaker (and broader) peak at 4000  $\text{cm}^{-1}$  was not revealed in the absorption measurements probably due to the weaker strength of this transition. We assign this peak to IVT from the ground HH1 subband of the QWs to the continuum of mixed (SO+LH) states above the barrier height. This would explain the high-energy shoulder of this peak that is expected to be weaker than bound to bound (or quasibound) transitions.

Another indication of the above assignments comes from measuring the polarization dependency of the photocurrent response. In Fig. 2(b) we show the response difference between  $p$ -polarized transverse magnetic (TM) and  $s$ -polarized transverse electric (TE) IR beams. Clearly, only the first peak at 1300  $\text{cm}^{-1}$ , which was assigned to heavy holes IST, is preferentially polarized along the growth direction as expected from the intersubband selection rules. The other transitions are not polarized at all as expected for IVTs.

The origin of the above transitions can be further investigated by plotting the integrated response, IRes, [i.e., the area below each peak in Fig. 2(a)] versus the bias voltage. This is shown in Fig. 3. The experimental data were fitted to a simple model where the voltage dependency of the integrated response is determined either by the drift velocity if bound to continuum transition is assumed, or by the drift velocity and tunneling through the extra energy barrier if bound to bound (or quasibound) transition is assumed.<sup>2</sup> The fitting procedure, shown by the solid lines in Fig. 3, indicate that the IST at 1300  $\text{cm}^{-1}$  is related to a bound to bound transition with the excited state located  $\sim$ 19 meV below the edge of the QWs. On the other hand, the IVT at 1800 and 2500  $\text{cm}^{-1}$  are related to bound to quasibound transition with effectively no barrier to tunnel. The most extreme situation occurs for the IVT at 4000  $\text{cm}^{-1}$  where the integrated response dependency on the bias voltage is very weak as expected for a bound to continuum transition. The best fitting to all peaks is obtained for a carrier's mobility of 600  $\text{cm}^2 \text{V}^{-1} \text{s}^{-1}$  in a good agreement with other mobility measurements in similar structures.<sup>16</sup>

In conclusion, the operation of a multispectral SiGe QWIP was demonstrated. This detector allows simultaneous detection at the LWIR, MWIR and SWIR atmospheric windows for TM polarization while only the MWIR and the SWIR bands can be detected if TE polarization is used. A very low dark current, comparable to GaAs QWIPs, was measured at bias voltages up to 5 V. We assign the improvement in the performances of the SiGe QWIP to the presence of a SiGe emitter and the use of a (relatively) low-temperature passivation process. We expect that using a larger number of SiGe QWs will further improve the absolute responsivity of the device and make it comparable to GaAs based QWIPs with some additional advantages for applications where the readout circuits and the QWIPs should monolithically be integrated.

<sup>1</sup>B. Levine, J. Appl. Phys. **74**, R1 (1993).

<sup>2</sup>K. K. Choi, *The Physics of Quantum Well Infrared Photodetectors* (World Scientific, Singapore, 1997).

<sup>3</sup>H. C. Liu, M. Buchanan, J. Li, Z. R. Wasilewski, P. H. Wilson, P. A. Marshall, R. A. Barber, P. Chow-Chong, J. W. Fraser, and J. Stapledon, *Applications of Photonic Technology 2*, edited by G. A. Lampropoulos

and R. A. Lessard (Plenum, New York, 1997), pp. 311–318.

<sup>4</sup>S. D. Gunapala, S. Bandara, J. K. Liu, W. Hong, M. Sundaram, R. Carralejo, C. A. Shott, P. D. Maker, and R. E. Muller, Proc. SPIE **3061**, 382 (1997).

<sup>5</sup>H. C. Liu, L. Li, J. R. Thompson, Z. R. Wasilewski, M. Buchanan, and J. G. Simmons, IEEE Electron Device Lett. **14**, 566 (1993).

<sup>6</sup>S. D. Gunapala, S. V. Bandara, A. Singh, J. K. Liu, E. M. E. M. Luong, J. M. Mumolo, and P. D. LeVan, Physica E (Amsterdam) **7**, 108 (2000).

<sup>7</sup>H. C. Liu, L. Li, M. Buchanan, Z. R. Wasilewski, G. J. Brown, F. Szmulowics, and S. M. Hegde, J. Appl. Phys. **83**, 585 (1998).

<sup>8</sup>S. S. Li and C. Y. H. Wang, Superlattices Microstruct. **19**, 229 (1996).

<sup>9</sup>R. P. G. Karunasiri, J. S. Park, and K. L. Wang, Appl. Phys. Lett. **59**, 2588 (1991); **61**, 2434 (1992).

<sup>10</sup>R. People, J. C. Bean, C. G. Bethea, S. K. Sputz, and L. J. Peticolas, Appl. Phys. Lett. **61**, 1122 (1992).

<sup>11</sup>P. Kruck, M. Helm, T. Fromherz, G. Bauer, J. F. Nutzel, and G. Abstreiter, Appl. Phys. Lett. **69**, 3372 (1996).

<sup>12</sup>T. Fromherz, E. Koppensteiner, M. Helm, G. Bauer, J. F. Nutzel, and G. Abstreiter, Phys. Rev. B **50**, 15073 (1994).

<sup>13</sup>R. People, IEEE J. Quantum Electron. **QE-22**, 1696 (1986).

<sup>14</sup>B. Adoram, D. Krapf, J. Shappir, A. Sa'ar, M. Levi, R. Beserman, S. G. Thomas, and K. L. Wang, Appl. Phys. Lett. **75**, 2232 (1999).

<sup>15</sup>B. Adoram, D. Krapf, M. Levi, R. Beserman, S. Thomas, K. L. Wang, J. Shappir, and A. Sa'ar, Physica E (Amsterdam) **7**, 255 (2000).

<sup>16</sup>Landödt-Bornstein, *Numerical Data Functional Relationships in Science and Technology*, New Series Group III, Vol. 17 (Springer, Berlin, 1982).